SDC Solenoid Design Note #153
EAR-30
August 15, 1991

A Stress Analysis of the Air Core Solenoid Conductor and Support Cylinder

Bob Wands

Introduction

The air core solenoid proposed by A. Yamamoto is subject to large axial compressive forces. This has prompted conductor development in Japan aimed at producing aluminum conductor capable of remaining in the elastic range under these large loads. Confidence in the solenoid could be increased if it can be shown that even a 'soft' conductor, such as that used in the CDF solenoid, would operate at an admissable level of strain in an air core solenoid. This work uses finite element magneto-structural analysis to examine the strains in the solenoid assuming the non-linear stress-strain behaviour of the CDF conductor, and compares them with the results of a similar analysis of the CDF solenoid.

Coil Geometry

The geometry of the air core solenoid is based on the Yamamoto design(1). A central field of 2 Tesla is assumed. The CDF detector geometry was available from Ref. 2, and the solenoid structural details were taken from Hitachi Drwg. #10P107-195.

Finite Element Models

A three-step finite element procedure was used in the analyses. First, a magnetostatic analysis was performed, using the meshes of Figs. 1 and 2. This analysis provided boundary conditions for a detailed submodels of the coils, shown in Figs. 3 and 4. This submodel was magnetostructural, coupling the Lorentz forces to the structural degrees of freedom to provide structural loads. However, at present the ANSYS magneto-structural coupling element does not allow plastic behaviour. Therefore, structural loads generated by the submodel were calculated as reaction forces by constraining all of the conductor structural degrees of freedom in the elements representing the Nb-Ti superconductor. These reaction forces were then converted to input for a strictly structural model based on the submodel mesh, but using an element which supports plastic behaviour.

The non-linear elastic option was used in ANSYS, since it is not load-path dependent but is equivalent to true plasticity provided no portion of the structure tends to unload (back down the stress-strain curve).

Two conductor characterizations were used for the air core analysis. The first was based on the CDF conductor stress-strain curve at 77 K [2], which is shown in Fig. 5. The second assumed that the conductor had the modulus of structural aluminum, and remained remained perfectly elastic during operation. This was implemented by equating the material properties of the support cylinder and conductor.

The CDF analysis assumed only the measured stress-strain curve for the conductor.

Isotropic material properties were assumed in all cases, i.e., the axial and hoop modulus of the conductor were equal.

Results

Table I compares the maximum conductor strain, stress intensity, and hoop and axial maximum stresses for the two SDC air core models, and from the CDF coil model.

Table I

	Air Core Elast. Strs/Strn Curve	Air Core CDF Strs/Strn Curve	CDF CDF Strs/Strn Curve
Coil Stress Intensity	62 MPa	42 MPa	34 MPa
Coil Strain	0.0009	0.0012	0.0007
Coil Hoop Stress	42 MPa	28 MPa	29 MPa
Coil Axial Stress	-20 MPa	-14 MPa	-5 MPa

Conclusion

The CDF conductor would achieve a strain of 0.0012 in/in if used in the air core solenoid. This is greater than the limit of 0.001 used in the CDF design. The CDF conductor would not be adequate for the SDC solenoid if it is an air core design with a maximum conductor strain limit of 0.001. A conductor with a yield strength high enough to remain in the elastic region under the loads assumed here, would be adequate.

References

1. Yamamoto, A., et. al.,'Progress on Design Study of the SDC Thin Superconducting Solenoid', draft presented at Fermilab meeting August 1, 1991.

2. Fast, R., et. al.,'Design Report for an Indirectly Cooled 3-m Diameter Superconducting Solenoid for the Fermilab Collider Detector Facility', TM-1135, October 1, 1982

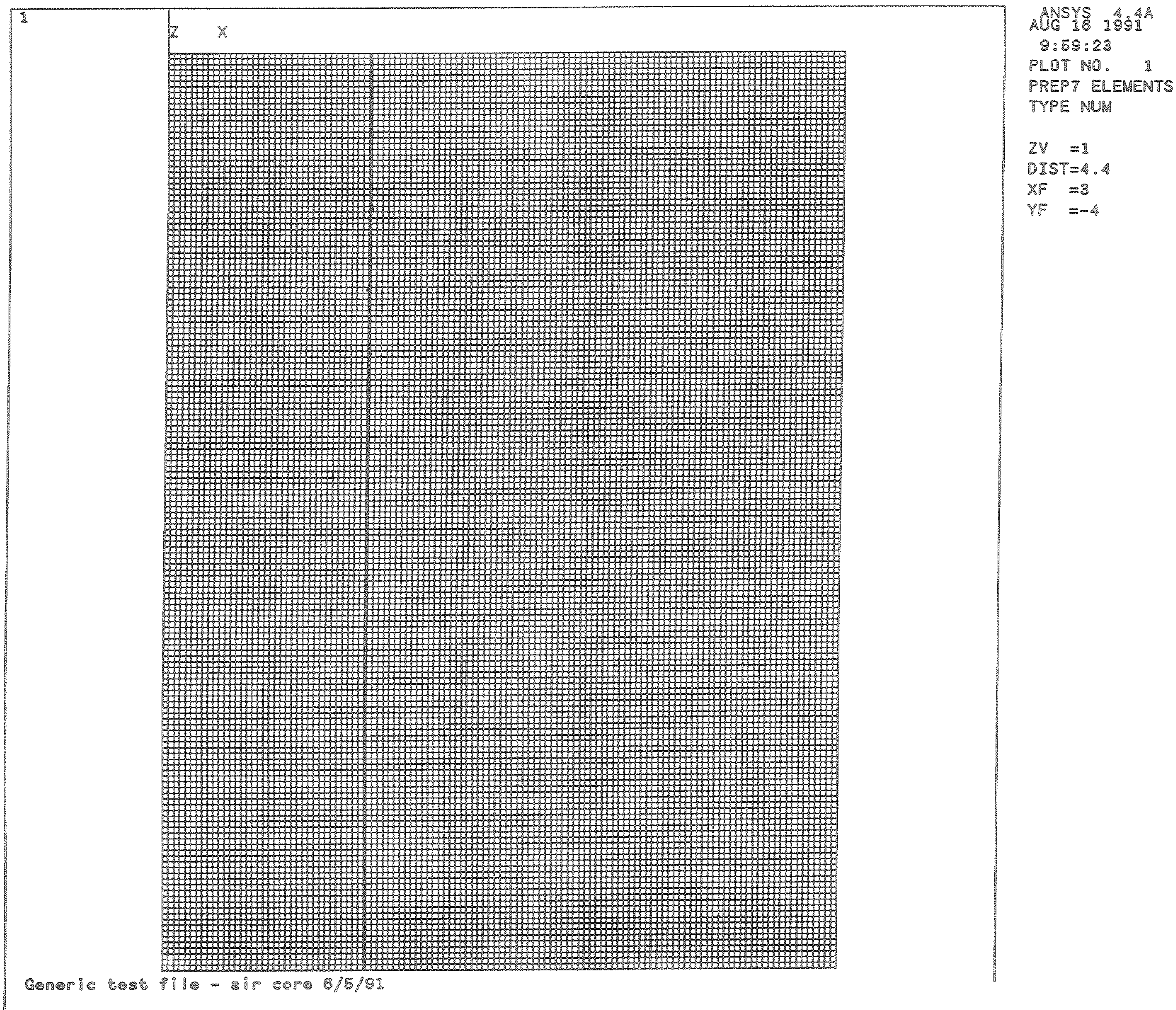

Fig. 1. Mesh for Air Core Solenoid Magnetostatic Analysis

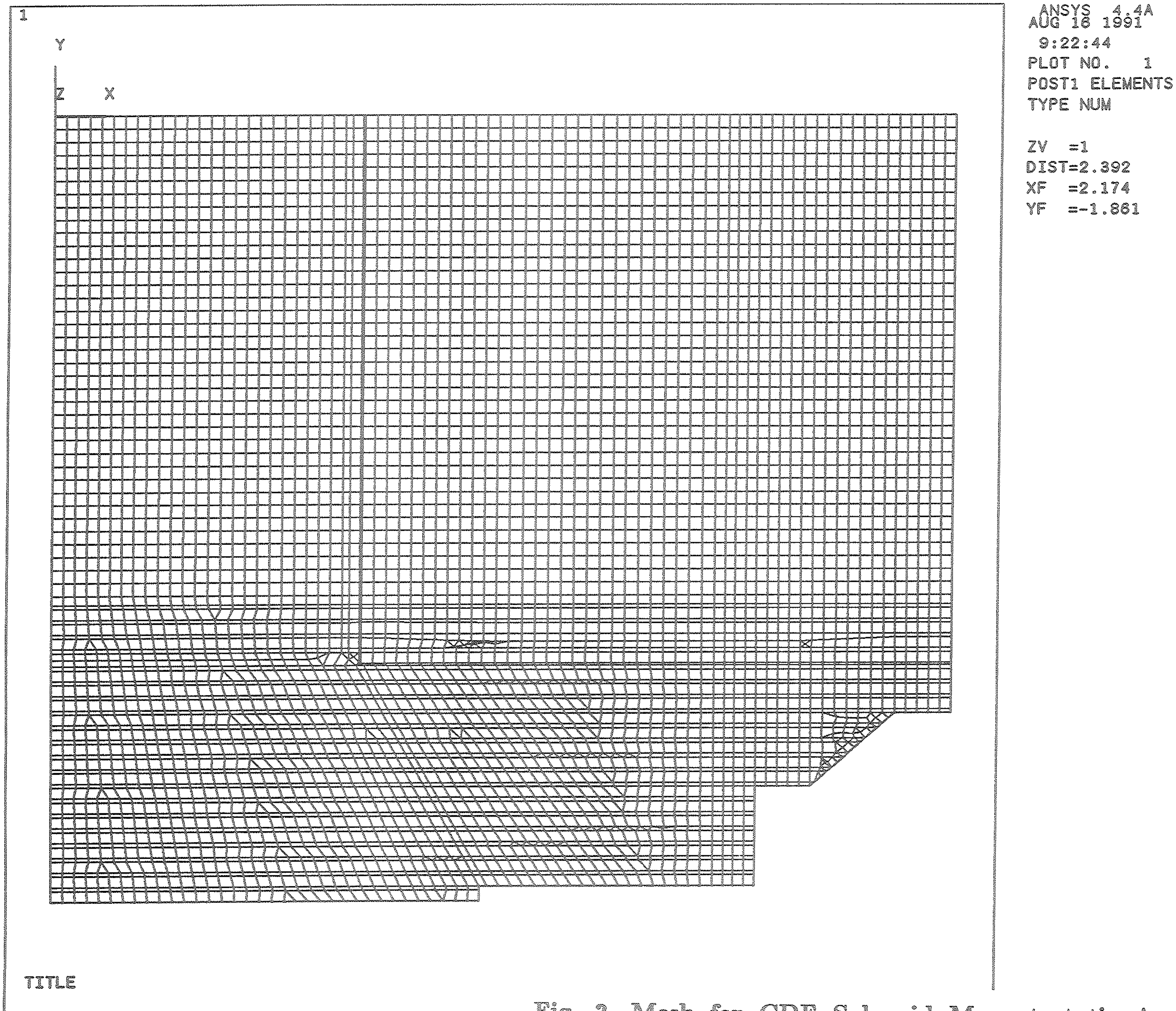

Fig. 2. Mesh for CDF Solenoid Magnetostatic Analysis

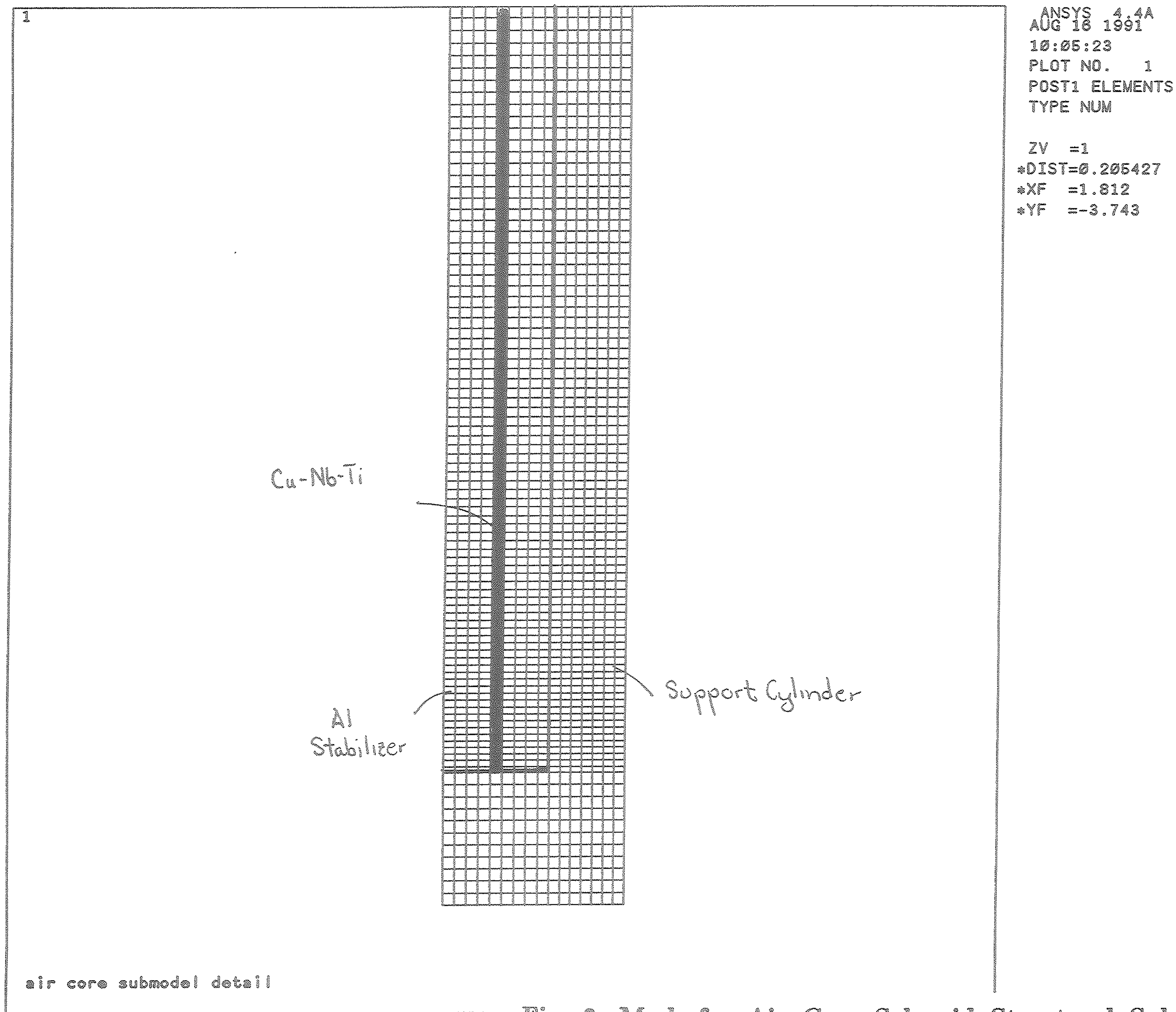

Fig. 3. Mesh for Air Core Solenoid Structural Submodel

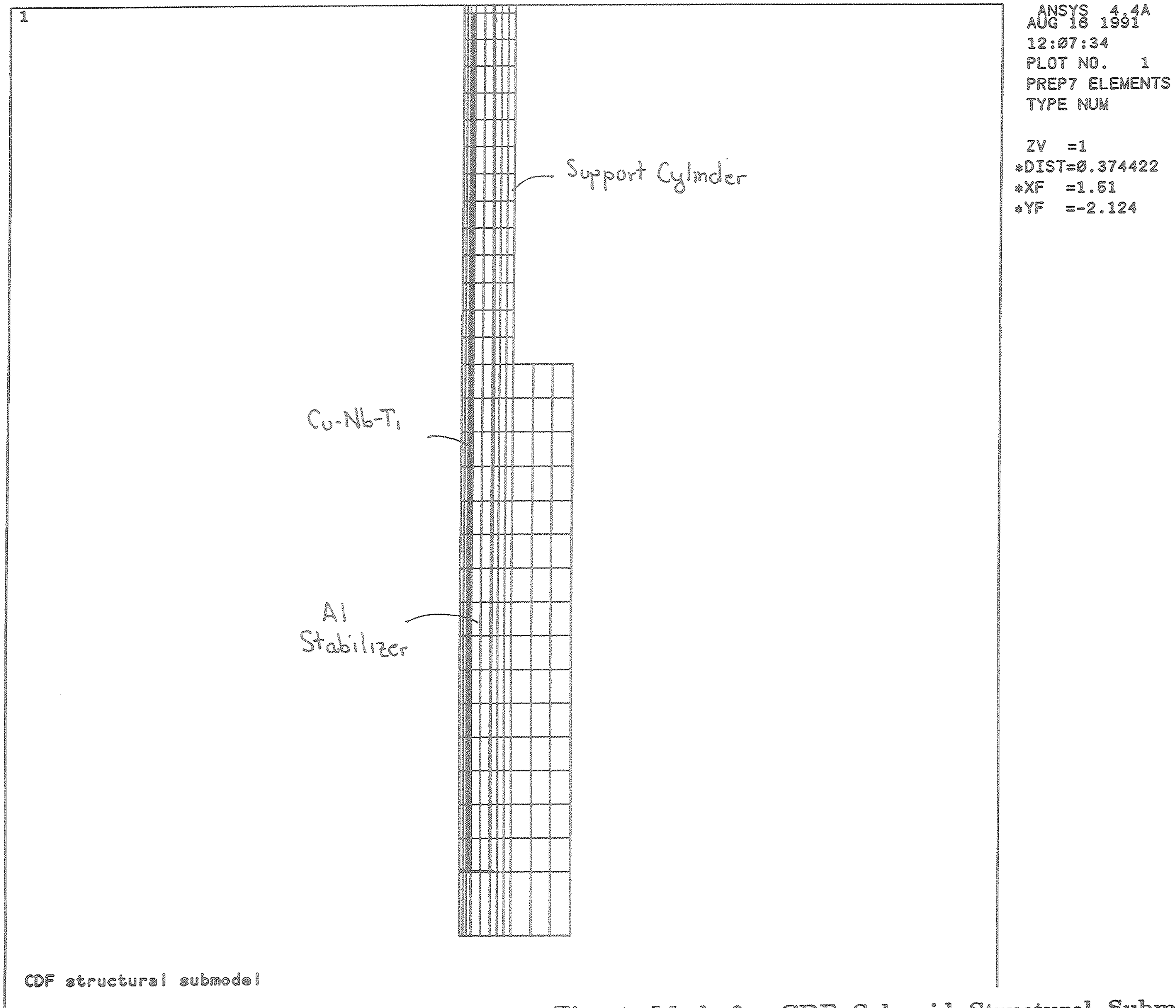

Fig. 4. Mesh for CDF Solenoid Structural Submodel

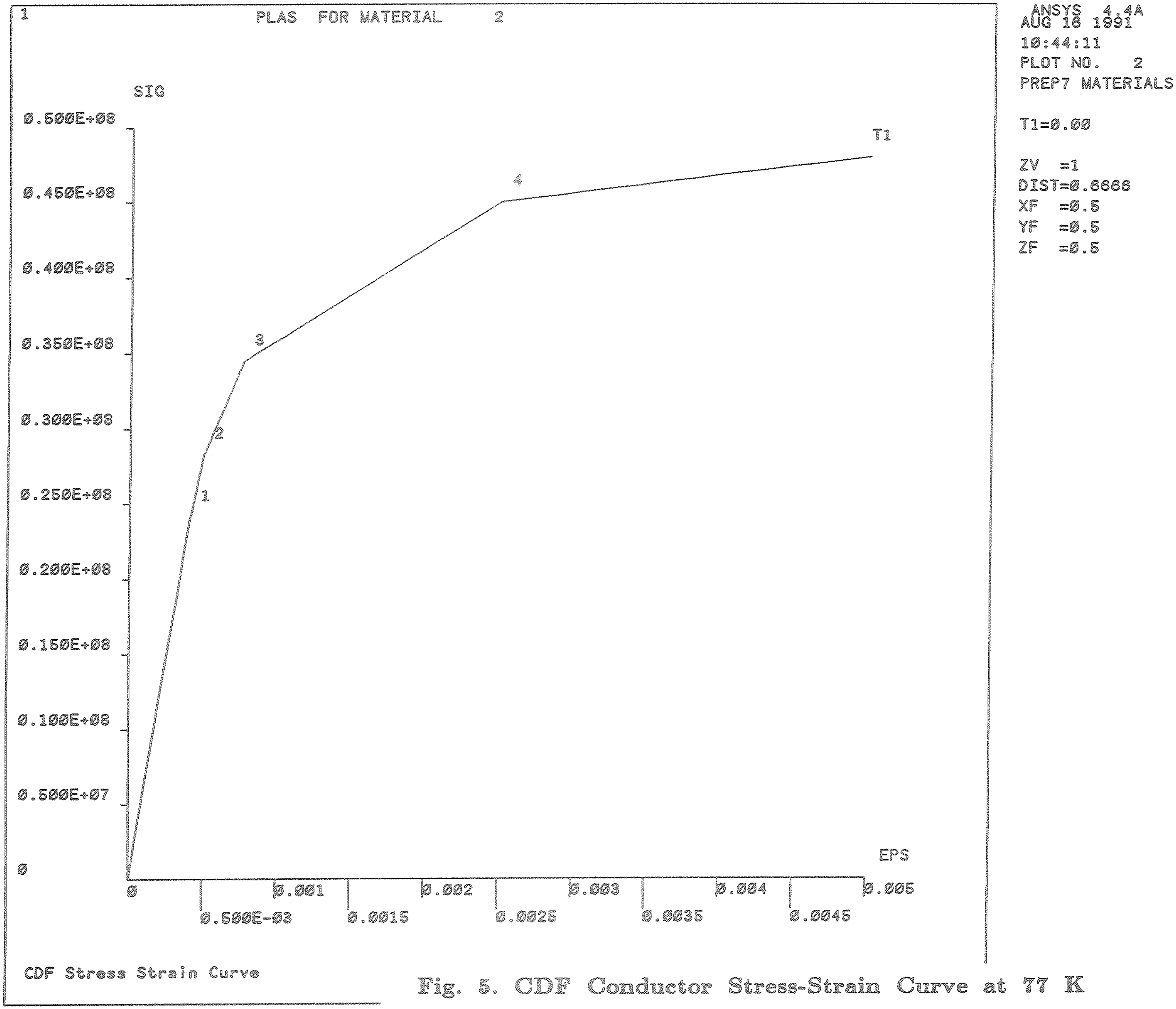

Fig. 5. CDF Conductor Stress-Strain Curve at 77 K